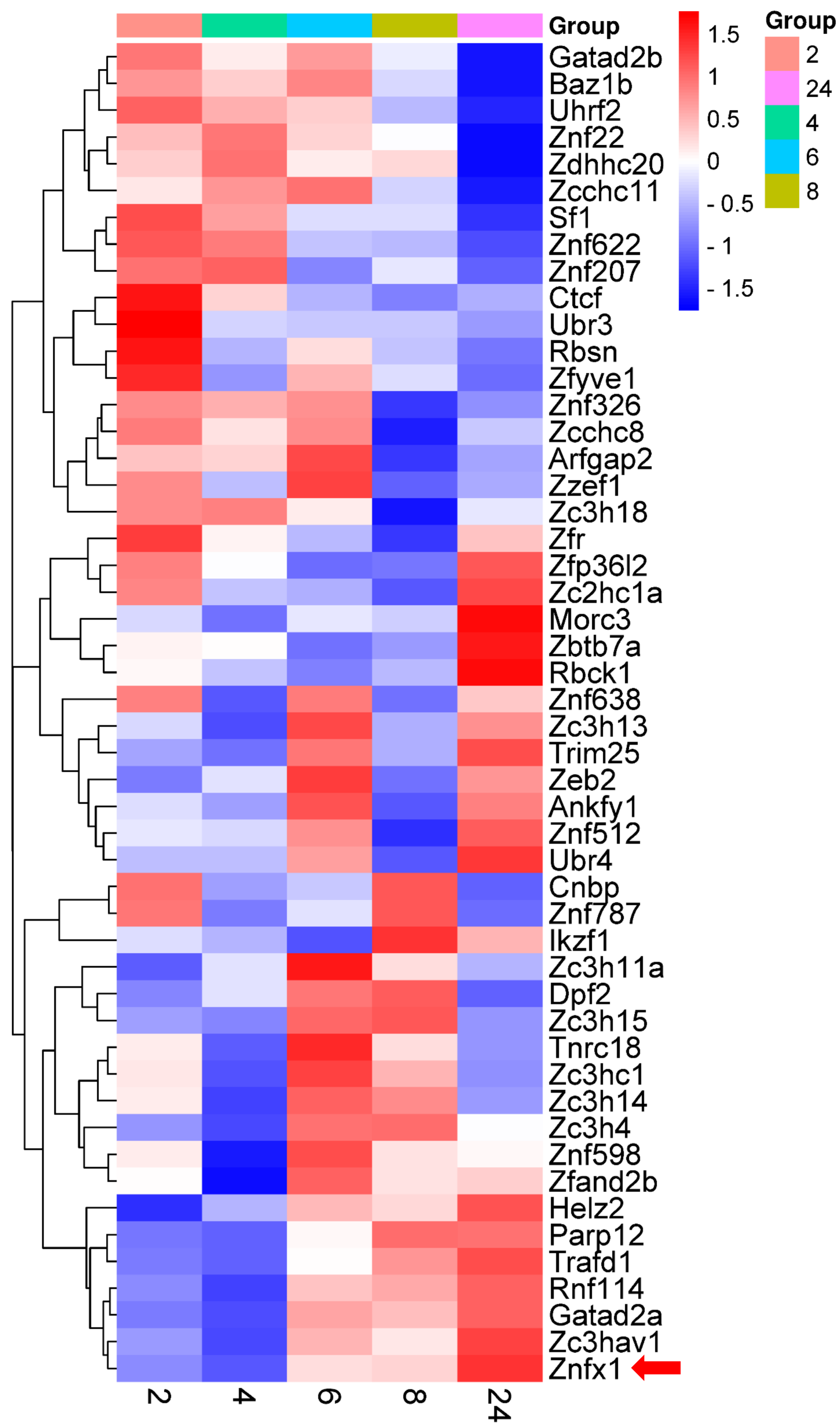
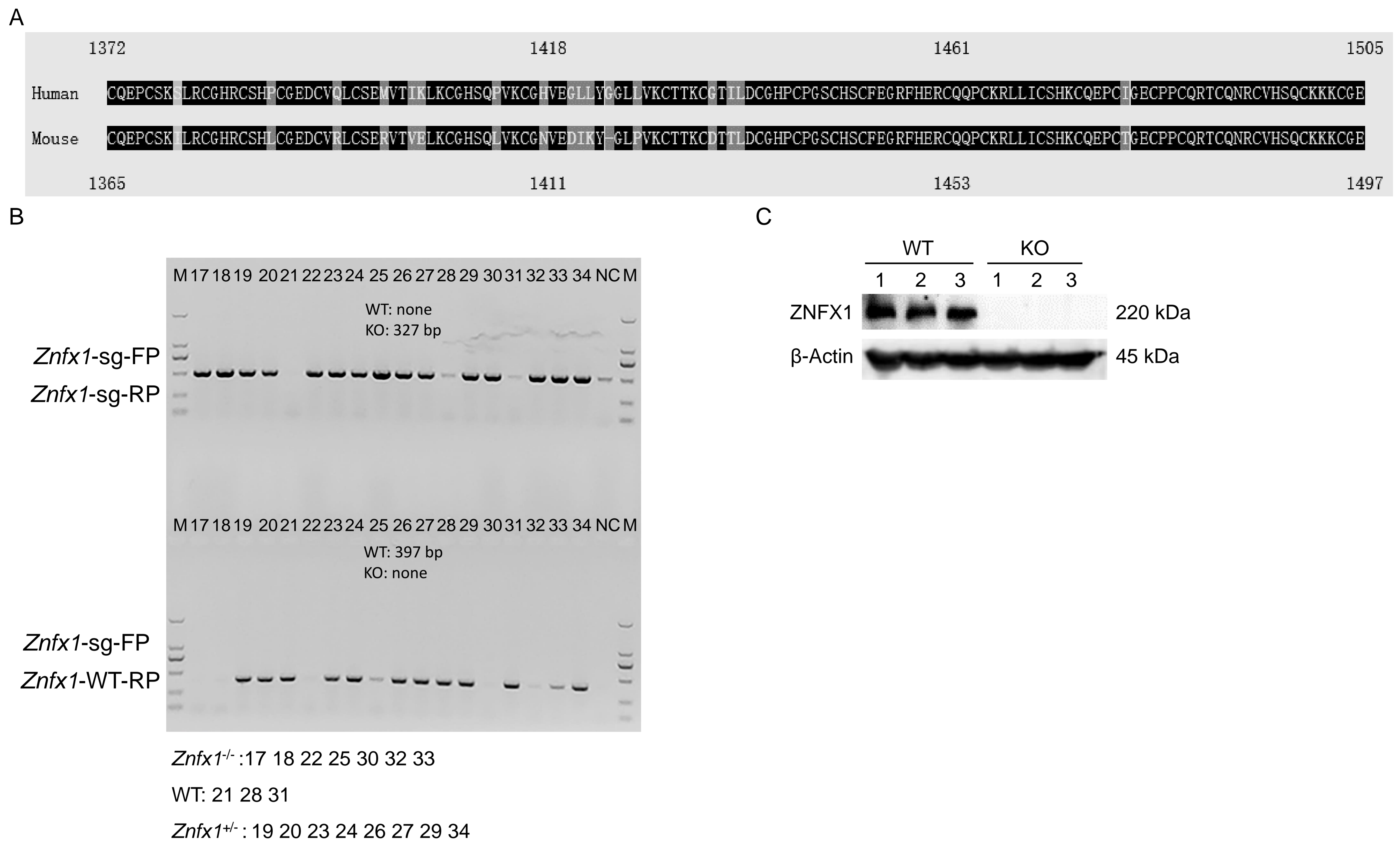


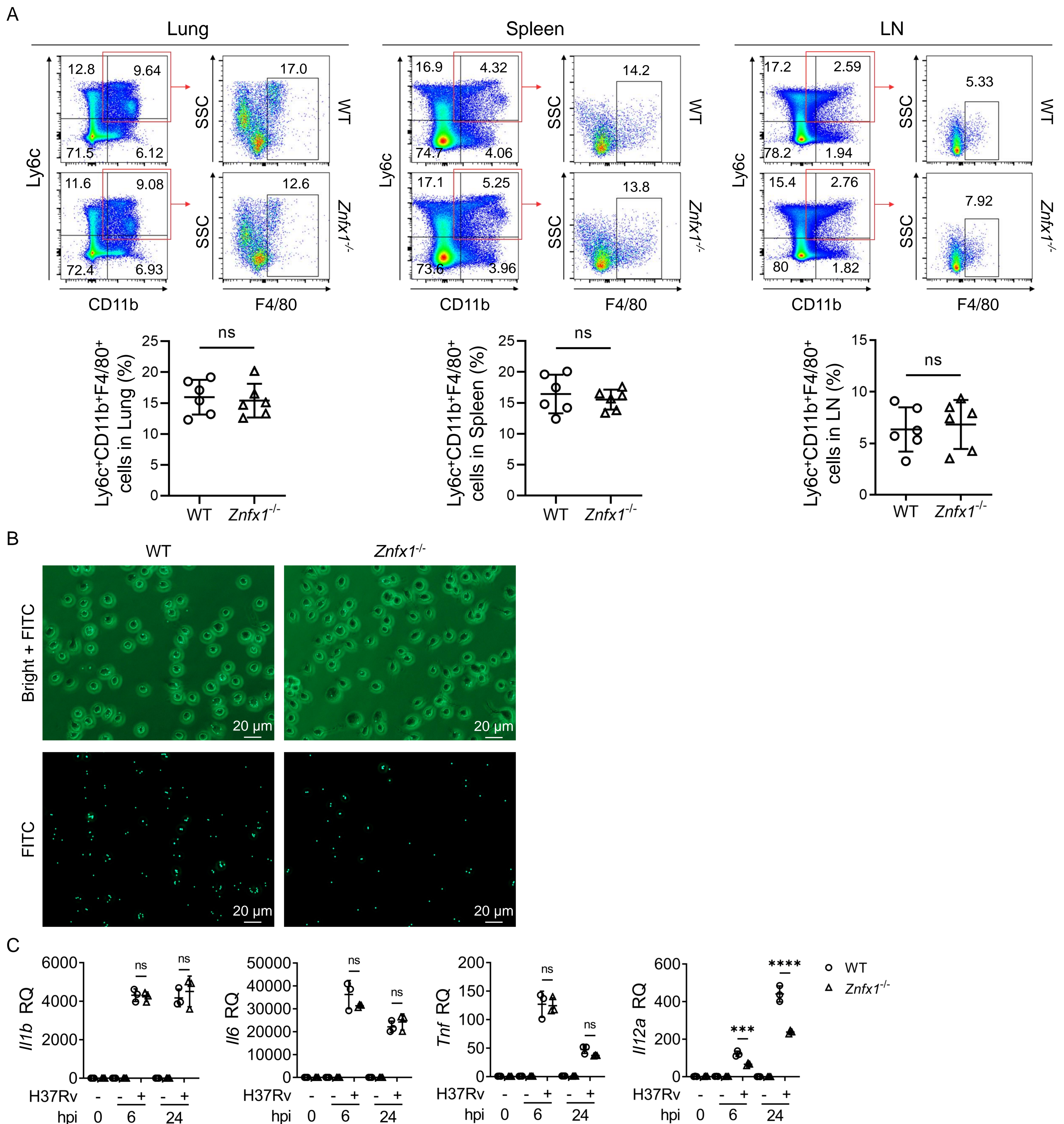
Supplementary Figures for ZNFX1



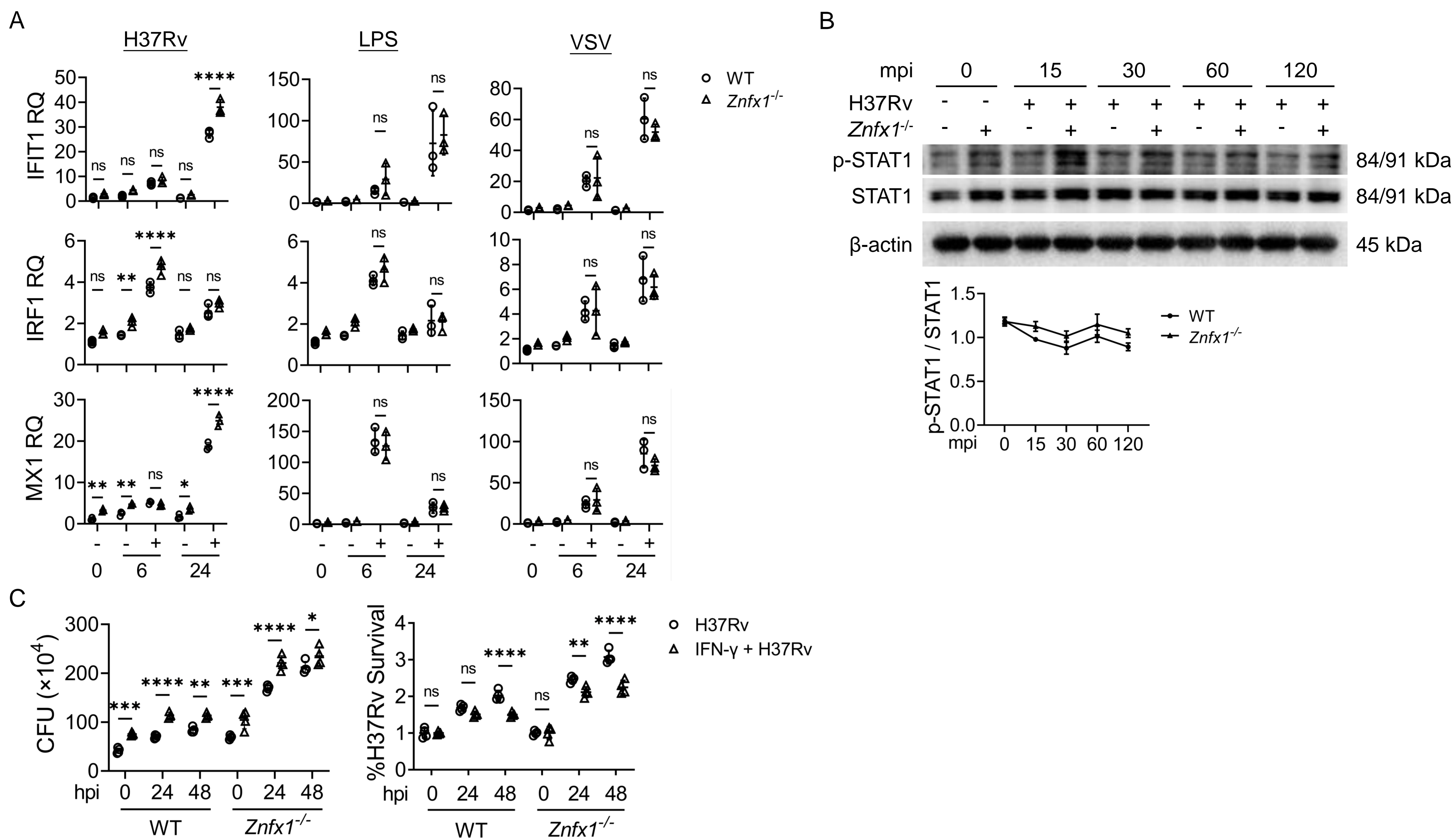
Supplementary Figure 1 for Figure 1. Heatmap of ZFP expression data from the study of Jonathan M. Budzik, et al. ¹⁸.



Supplementary Figure 2 for Figure 2. Sequence alignment of human and murine ZNF1 proteins, and Identification of *Znf1*^{-/-} mice. (A) Sequence alignment of the zinc finger region of human and murine ZNF1 proteins. (B-C) Identification of *Znf1*^{-/-} mice using PCR (B) and western blotting (C).

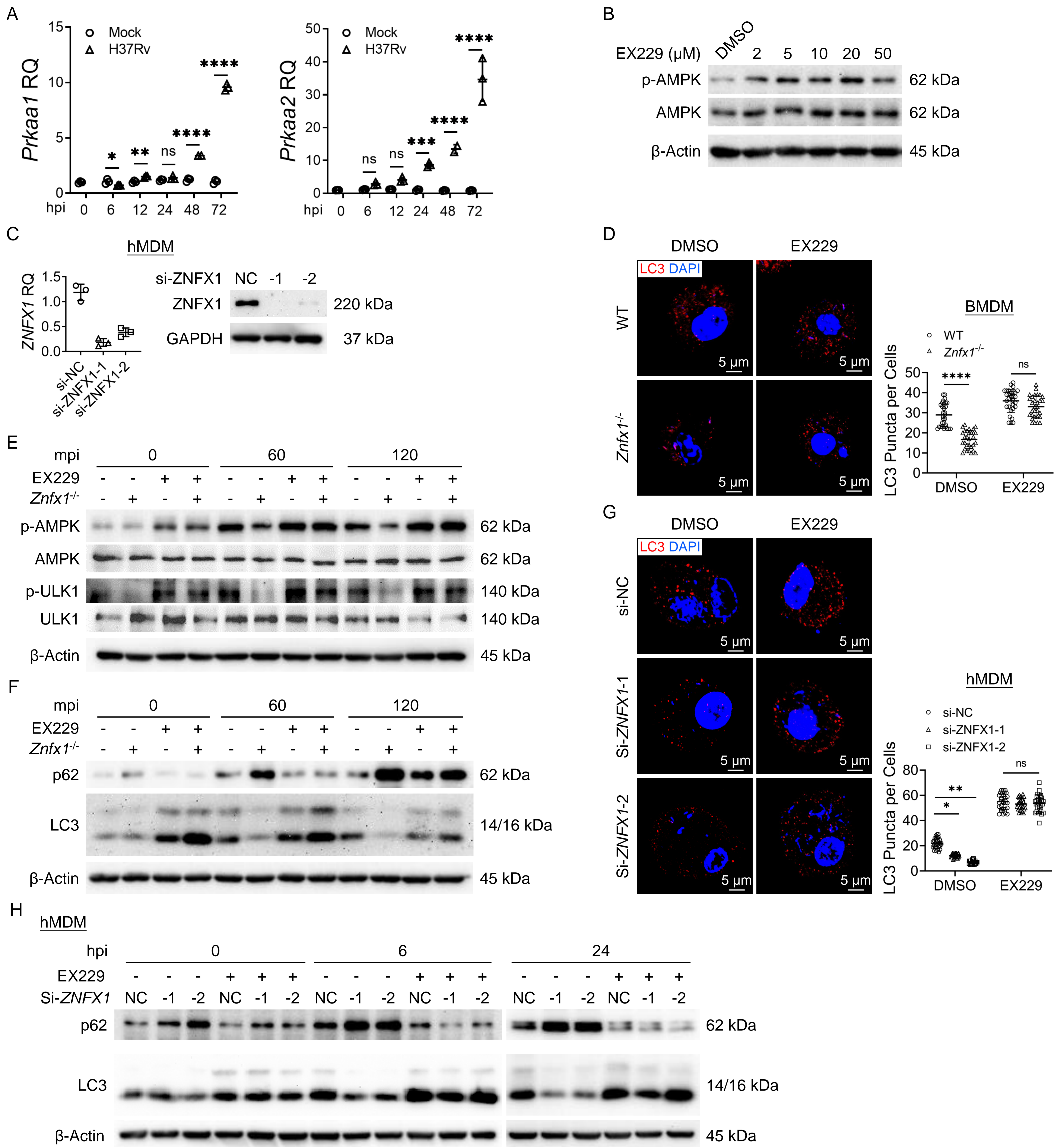


Supplementary Figure 3 for Figure 3. Amount and activity of *Znf1*^{-/-} Mφ. **(A)** Flow cytometry analysis of Ly6C⁺CD11b⁺F4/80⁺ Mφ amounts in the lung, spleen and LN of WT and *Znf1*^{-/-} mice (*n* = 6). **(B)** Fluorescent photographs of green fluorescence positive WT and *Znf1*^{-/-} BMDMs incubated with FITC-conjugated Latex. **(C)** qPCR detection of cytokine expression in *Znf1*^{-/-} BMDMs infected with H37Rv (*n* = 3). An unpaired *t* test (A) and a two-way ANOVA with Šidák's post hoc test (C) was used for statistical analysis. Data are presented as mean ± SD and are representative of at least three experiments with similar observations. **P* < 0.05; ***P* < 0.01; ****P* < 0.001; *****P* < 0.0001.

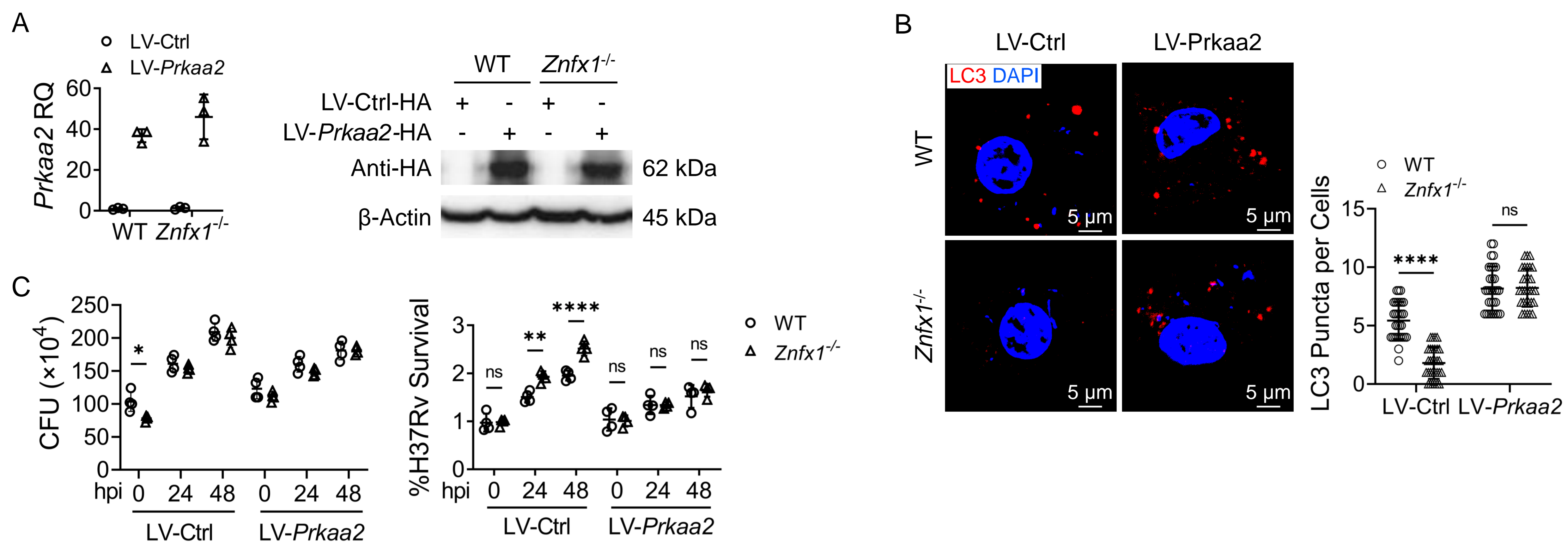


Supplementary Figure 4 for Figure 3. The ISG signaling pathway did not mediate the function of ZNFX1 in response to Mtb infection. **(A)** RT-PCR detection of ISG expression in *Znfx1*^{-/-} BMDMs following stimulation with H37Rv, LPS and VSV, respectively ($n = 3$). **(B)** Western blot assay of activation of STAT1 in H37Rv-infected *Znfx1*^{-/-} BMDMs. The relative levels of STAT1 phosphorylation was quantified ($n = 3$). **(C)** CFU assays of Mtb load in *Znfx1*^{-/-} BMDMs treated with or without IFN- γ ($n = 4$). A two-way ANOVA with Šidák's post hoc test (A and C) was used for statistical analysis. Data are presented as mean \pm SD and are representative of at least three experiments with similar observations. * $P < 0.05$; ** $P < 0.01$; *** $P < 0.001$; **** $P < 0.0001$.

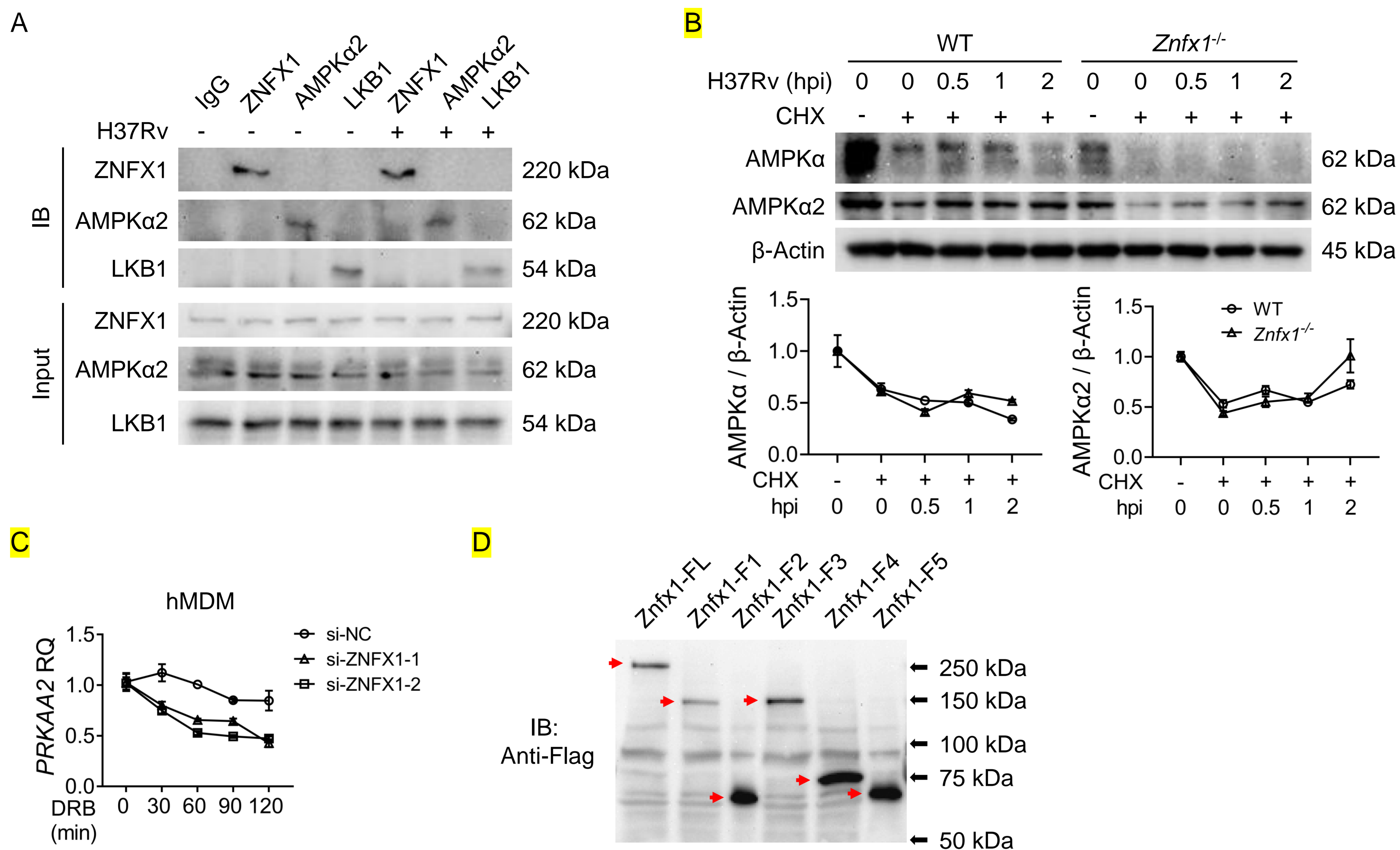
Supplementary Figure 5



Supplementary Figure 5 for Figure 5. Recovery of AMPK α activation or expression promoted autophagy and bactericidal activity of M ϕ resulted from absence of ZNFX1. **(A)** RT-PCR detection of *Prkaa1* and *Prkaa2* expression in H37Rv-infected *Znfx1*^{-/-} BMDMs. **(B)** Western blot assay of AMPK activation following EX229 treatment of BMDMs. **(C)** RT-PCR and Western blot assay of ZNFX1 silencing in hMDMs. **(D)** Immunofluorescence staining of LC3 in H37Rv-infected *Znfx1*^{-/-} BMDMs following EX229 treatment (30 randomly selected cells for statistics). **(E-F)** Western blot assay of activation of AMPK and downstream ULK1 **(E)**, p62 level and LC3 conversion **(F)** in EX229-treated *Znfx1*^{-/-} BMDMs followed by H37Rv infection ($n = 3$). **(G)** Immunofluorescence staining of LC3 in H37Rv-infected ZNFX1-silencing hMDMs following EX229 treatment (30 randomly selected cells for statistics). **(H)** Western blot assay of p62 level and LC3 conversion in EX229-treated ZNFX1-silencing hMDMs followed by H37Rv infection ($n = 3$). A two-way ANOVA with Šidák's post hoc test (A, D and G) was used for statistical analysis. Data are presented as mean \pm SD and are representative of at least three experiments with similar observations. * $P < 0.05$; ** $P < 0.01$; *** $P < 0.001$; **** $P < 0.0001$.



Supplementary Figure 6 for Figure 5. Recovery of AMPK α expression promoted autophagy and bactericidal activity of M ϕ resulted from absence of ZNF1. **(A)** RT-PCR and western blot assay of overexpression of *Prkaa2* in *Znf1*^{-/-} BMDMs ($n = 3$). **(B)** Immunofluorescence staining of LC3 in H37Rv-infected *Znf1*^{-/-} BMDMs overexpressing *Prkaa2* (30 randomly selected cells for statistics). **(C)** CFU assay of Mtb load in *Znf1*^{-/-} BMDMs overexpressing *Prkaa2* ($n = 4$). A two-way ANOVA with Šidák's post hoc test (B and C) was used for statistical analysis. Data are presented as mean \pm SD and are representative of at least three experiments with similar observations. * $P < 0.05$; ** $P < 0.01$; *** $P < 0.001$; **** $P < 0.0001$.



Supplementary Figure 7 for Figure 7. *In vitro* and *in vivo* experiments confirming that *Prkaa2* mediated the function of ZNFX1. **(A)** IP experiment and western blot assay of combination among ZNFX1, AMPK α 2 and LKB1. **(B)** Western blotting of AMPK α and AMPK α 2 in *Znfx1^{-/-}* BMDMs treated with CHX, with analysis of protein degradation rates ($n = 3$). **(C)** qPCR analysis of *PRKAA2* in *ZNFX1*-silenced hMDMs treated with DRB ($n = 3$). **(D)** Western blot assay of full length or various truncated forms of ZNFX1 expression in 293T cells. A two-way ANOVA with Šidák's post hoc test (B and C) was used for statistical analysis. Data are presented as mean \pm SD and are representative of at least three experiments with similar observations. * $P < 0.05$; ** $P < 0.01$; *** $P < 0.001$; **** $P < 0.0001$.